

Hyperspherical theory of anisotropic exciton

E. A. Muljarov,^{*} A. L. Yablonskii, and S. G. Tikhodeev

General Physics Institute, RAS, Moscow 117942, Vavilov st., 38, Russia

A. E. Bulatov and Joseph L. Birman

Physics Department, City College of New York, New York, NY 10031

(Dated: November 6, 2018)

Abstract

A new approach to the theory of anisotropic exciton based on Fock transformation, i.e., on a stereographic projection of the momentum to the unit 4-dimensional (4D) sphere, is developed. Hyperspherical functions are used as a basis of the perturbation theory. The binding energies, wave functions and oscillator strengths of elongated as well as flattened excitons are obtained numerically. It is shown that with an increase of the anisotropy degree the oscillator strengths are markedly redistributed between optically active and formerly inactive states, making the latter optically active. An approximate analytical solution of the anisotropic exciton problem taking into account the angular momentum conserving terms is obtained. This solution gives the binding energies of moderately anisotropic exciton with a good accuracy and provides a useful qualitative description of the energy level evolution.

I. INTRODUCTION

The interest to the anisotropic exciton problem^{2,3} has been revived with the progress in the physics of semiconductor heterostructures. In semiconductor superlattices the miniband formation causes a strong mass anisotropy.⁴ In fact, the localization of carriers inside quantum wells and their tunneling through barriers can be described in terms of anisotropic medium approximation as the effect of mass renormalization. The dielectric constant becomes anisotropic also if the superlattice constituent layers have different dielectric susceptibilities. Recently such a formalism has been used in the theory of excitons in short-period superlattices (see, e.g., Refs. 5,6).

The main complication of the uniaxial anisotropic exciton problem is that the Coulomb potential symmetry is broken (the spherical symmetry as well as the “hidden” one, the intrinsic property of the hydrogen-like system) so that only the angular momentum projection and parity conserve. As a consequence, the solution of the Schrödinger equation is no more factorized into radial and angular parts and cannot be represented as a finite combination of standard special functions.

The anisotropic exciton problem was first studied by Kohn and Luttinger³ (for donor states in silicon and germanium) by means of the variational approach with allowance for a group symmetry of the particular materials. Further theoretical studies^{7–17} were focused on perturbative solutions of the anisotropic exciton problem. For slightly anisotropic system Hopfield and Thomas⁷ found the first-order solution, treating the anisotropy of the kinetic energy as a perturbation¹⁸ linear in the anisotropy parameter. The effects in a weak magnetic field also have been taken into account in this approximation. For a moderate exciton anisotropy Wheeler and Dimmock⁸ used an expansion of the anisotropic potential over its asymmetric part z^2/r^2 up to the second order in the anisotropy parameter terms, thus calculating in part the second-order perturbation solution. This partial diagonalization was completed by Deverin,⁹ who considered the diagonal elements of the exact anisotropic kinetic energy (for nondegenerate levels) as well as the transcendental solution of a secular problem for degenerate levels. The full expansion of the anisotropic potential was considered by Segal¹⁰, where only the spherically symmetric part of the full expansion was taken into account. Finally, Faulkner¹¹ performed calculations of donor energy levels by means of Rayleigh-Ritz perturbation method containing numerous (depending on hydrogen

quantum numbers) variational parameters. Being included in the radial part of hydrogen basis functions, these variational parameters served as scaling factors depending on the anisotropy degree. In the limit of an extreme anisotropy, the exciton binding energies were calculated^{3,12,13} in adiabatic approximation. Following the method suggested by Faulkner, Baldereschi and Diaz¹⁴ obtained similar results and attempted to calculate excitonic oscillator strengths. The same Rayleigh-Ritz method was used in Ref. 17 for calculations of the energy levels of 2D anisotropic exciton.

Recently, an elegant model of fractional-dimensional space has been developed [see Refs. 19,20 and references therein]. It allows to treat self-consistently the bound as well as continuum states in hydrogen problem of noninteger dimension. However, its direct applicability to the anisotropic exciton problem is problematic. The reason is that the fractional-dimensional hydrogen problem conserves the Coulomb degeneracy of levels (so that the binding energies depend on the principal quantum number only), whereas in reality the anisotropy lifts this degeneracy and restores it only in 2D and 3D cases.

In spite of a long history of theoretical study, the investigation of the optical properties of the anisotropic exciton is still not complete. For example, the behavior of exciton oscillator strengths is very important for the understanding the experimental absorption spectra. However, the evolution of the oscillator strengths of the anisotropic exciton with the increase of the anisotropy has not been investigated, for our knowledge, with two exceptions: calculations for slightly anisotropic exciton¹⁴ and simulations of optical spectra within an isotropic exciton model.²¹ One should note that none of the approaches^{14,21} is able to describe the drastic changes of oscillator strengths (due to the level anticrossings¹¹) with increase of the anisotropy reported in our paper.

In the present paper we develop²² a perturbation approach to the uniaxial anisotropic exciton problem, based on the method of stereographic projection of the momentum space to the unit 4D-sphere, proposed by Fock.²³ We use the hyperspherical harmonics, i.e., the irreducible representation of rotation group $O(4)$ of a 4D-sphere, as a basis of Brillouin-Wigner perturbation method.

This approach has a number of advantages and clarifies the physical properties of the anisotropic exciton. (i) It allows us to utilize the additional hidden symmetry of Coulomb potential for expansion of anisotropic exciton wave function. Namely, for the bound exciton states the irreducible representation of the full symmetry group $O(4)$ constitutes a complete

set for such expansion. This expansion depends explicitly on the exciton energy through scaling parameters which follow adiabatically the changes in anisotropy. These parameters, similar to those introduced in the Rayleigh-Ritz method¹¹ (where they were defined by minimizing the energy functional) are exactly determined in our method. As a result, the hyperspherical functions turn out to be the most effective basis for numerical calculations. (ii) Within Fock representation, the hydrogenic spectrum with the level series limit transforms into an equidistant one, which provides a good convergence of our method in a wide region of the anisotropy parameter. (iii) The matrix elements of the perturbation are found as analytical elementary expressions. (iv) This analytical form of perturbation matrix elements allows us to construct a spherical approximation with an analytical solution and to summarize exactly the rest part of perturbation in the second order. This spherical approximation, which works well in the region of a moderate anisotropy, turns out to be very useful for qualitative classification of the energy levels.

We calculate numerically the energy spectrum, excitonic wavefunctions and oscillator strengths for flattened as well as elongated excitons.

The paper is organized as follows. In Sec. II the expansion is formulated on the basis of hyperspherical formalism and basic equations of the perturbation method are derived. Results and discussions are presented in Sec. III.

II. ANISOTROPIC EXCITON IN FOCK REPRESENTATION

A. Hyperspherical formalism

The Hamiltonian of the uniaxial anisotropic exciton is given by

$$\hat{H} = -\frac{\hbar^2}{2\mu_{\perp}} \left(\frac{\partial^2}{\partial x^2} + \frac{\partial^2}{\partial y^2} \right) - \frac{\hbar^2}{2\mu_{\parallel}} \frac{\partial^2}{\partial z^2} - \frac{e^2}{\sqrt{\varepsilon_{\parallel}\varepsilon_{\perp}(x^2 + y^2) + \varepsilon_{\perp}^2 z^2}}. \quad (1)$$

Here μ is the reduced exciton mass, ε is the semiconductor dielectric constant, and subscripts \parallel and \perp refer to the quantities along and normal to the axis of symmetry (z -axis), respectively. In Eq. (1) both the kinetic and potential energies are anisotropic. However, a dilatation $z \rightarrow z\sqrt{\varepsilon_{\parallel}/\varepsilon_{\perp}}$ makes the potential energy spherically symmetric. In the effective atomic units

$$\text{Ry}^* = \frac{\mu_{\perp} e^4}{2\varepsilon_0^2 \hbar^2}, \quad a_{\text{B}}^* = \frac{\hbar^2 \varepsilon_0}{\mu_{\perp} e^2}, \quad (2)$$

where $\varepsilon_0 = \sqrt{\varepsilon_\perp \varepsilon_\parallel}$, Eq. (1) takes the form

$$\left(\hat{\mathbf{p}}^2 + \epsilon \hat{p}_z^2 - \frac{2}{r} \right) \psi(\mathbf{r}) = E \psi(\mathbf{r}). \quad (3)$$

Here we introduced the perturbation parameter, $\epsilon = \gamma - 1$, connected to the anisotropy parameter,

$$\gamma = \frac{\varepsilon_\perp \mu_\perp}{\varepsilon_\parallel \mu_\parallel} \quad (4)$$

($0 < \gamma < 1$ and $1 < \gamma < \infty$ for, respectively, flattened and elongated exciton), $\hat{\mathbf{p}}$ and \hat{p}_z denote, respectively, the dimensionless operators of momentum and its z -projection.

We investigate the bound states with eigenenergies $E_\nu < 0$, measured in Ry^* , Eq. (2). It is convenient to introduce a parameter (for each bound states ν)

$$p_\nu = \sqrt{-E_\nu}, \quad (5)$$

which will play the role of the adiabatic parameter in the perturbation theory. After the Fourier transform, Eq. (3) takes the integral form

$$(p^2 + \epsilon p_z^2 + p_\nu^2) \psi_\nu(\mathbf{p}) = \frac{1}{2\pi^2} \int \frac{\psi_\nu(\mathbf{p}')}{|\mathbf{p} - \mathbf{p}'|^2} d^3 p'. \quad (6)$$

Following Fock's paper,²³ we perform a stereographic projection of 3D momentum space to the 4D unit sphere, $\mathbf{p}/p_\nu \rightarrow \vec{u}$, where the 4D vector \vec{u} on the sphere is defined as

$$\vec{u} = \{\mathbf{u}, u_n\} = \left\{ \frac{2p_\nu \mathbf{p}}{p^2 + p_\nu^2}, \frac{p^2 - p_\nu^2}{p^2 + p_\nu^2} \right\}, \quad (7)$$

$p = |\mathbf{p}|$. In the hyperspherical coordinates, $(\alpha, \theta, \varphi)$, the unit vector \vec{u} takes the form

$$\left\{ \begin{array}{l} u_x = \frac{2p_\nu p_x}{p^2 + p_\nu^2} = \sin \alpha \sin \theta \cos \varphi, \\ u_y = \frac{2p_\nu p_y}{p^2 + p_\nu^2} = \sin \alpha \sin \theta \sin \varphi, \\ u_z = \frac{2p_\nu p_z}{p^2 + p_\nu^2} = \sin \alpha \cos \theta, \\ u_n = \frac{p^2 - p_\nu^2}{p^2 + p_\nu^2} = \cos \alpha, \end{array} \right. \quad (8)$$

and

$$d^4 \Omega = \sin^2 \alpha d\alpha \sin \theta d\theta d\varphi = \frac{8p_\nu^3}{(p^2 + p_\nu^2)^3} d^3 p. \quad (9)$$

Let us introduce a new wave function

$$\Psi_\nu(\vec{u}) = \frac{(p^2 + p_\nu^2)^2}{4p_\nu^{5/2}} \psi_\nu(\mathbf{p}), \quad (10)$$

with normalization condition

$$\int |\psi_\nu(\mathbf{p})|^2 d^3p = \int (1 - \cos \alpha) |\Psi_\nu(\vec{u})|^2 d^4\Omega = 1. \quad (11)$$

Then Eq. (6) takes the form

$$\left(1 + \frac{\epsilon}{2} \hat{V}\right) \Psi_\nu(\vec{u}) = \frac{1}{p_\nu} \hat{H}_0 \Psi_\nu(\vec{u}). \quad (12)$$

Here \hat{H}_0 is the Hamiltonian of unperturbed (hydrogen-like) problem,

$$\hat{H}_0 \Psi(\vec{u}) = \frac{1}{2\pi^2} \int \frac{\Psi(\vec{u}')}{|\vec{u} - \vec{u}'|^2} d^4\Omega', \quad (13)$$

and \hat{V} is the perturbation operator,

$$\hat{V} = \frac{u_z^2}{1 - u_n} = (1 + \cos \alpha) \cos^2 \theta. \quad (14)$$

If $\epsilon = 0$ (or $\gamma = 1$), Eq. (12) describes the isotropic 3D exciton. As it was shown by Fock,²³ the solutions of the integral equation

$$\Psi^{(0)} = \lambda^{(0)} \hat{H}_0 \Psi^{(0)} \quad (15)$$

are

$$\Psi_{nlm}^{(0)}(\alpha, \theta, \varphi) = (-2i)^l l! \sqrt{\frac{2n(n-l-1)!}{\pi(n+l)!}} \sin^l \alpha C_{n-l-1}^{l+1}(\cos \alpha) Y_{lm}(\theta, \varphi), \quad (16)$$

$$\lambda_{nlm}^{(0)} = n, \quad n = 1, 2, \dots, \quad l = 0, \dots, n-1, \quad m = 0, \pm 1, \dots, \pm l. \quad (17)$$

Here $C_k^m(x)$ are the Gegenbauer polynomials²⁴ and $Y_{lm}(\theta, \varphi)$ are the conventional spherical harmonics. The hyperspherical functions, Eq. (16), afford the irreducible representation of the full symmetry group $O(4)$ of the hydrogen-like system.²⁵ Due to the properties of irreducible representations, the hyperspherical function are orthogonal and normalized as

$$\int |\Psi_{nlm}^{(0)}(\alpha, \theta, \varphi)|^2 d^4\Omega = \int (1 - \cos \alpha) |\Psi_{nlm}^{(0)}(\alpha, \theta, \varphi)|^2 d^4\Omega = 1, \quad (18)$$

in accordance²⁶ with Eq. (11). It can be shown²⁷ that the standard hydrogen wave function $\phi_{nlm}^{(0)}(\mathbf{r})$ with a given set of quantum numbers (n, l, m) (see, e.g., in Ref. 28) can be Fourier transformed into the hyperspherical function, Eq. (16).

B. Formulation of Brillouin-Wigner perturbation theory

We use the Brillouin-Wigner perturbation theory, i.e. the direct diagonalization of a truncated Hamiltonian matrix in order to solve the anisotropic exciton problem in the form of Eq. (12). The set of the hydrogen bound states eigenfunctions is not complete and the scattering states also must be taken into account. However, in Fock representation we are able to construct a complete basis out of the set of the hydrogen bound states. As it was shown in Ref. 25, the scattering states are mapped on a two-sheeted hyperboloid in a 4D space with Minkowski metrics, whereas the bound states are mapped into a unit sphere via the transformation Eq. (8). Thus, the problems of the bound and scattering states are mapped onto different subspaces, each of them to have its own complete basis. The anisotropic problem is mapped into the same subspaces through the transformation Eqs. (7)–(10) for the bound states and the corresponding procedure (with positive energies) for the scattering states. So, being interested in bound states in the whole physical region $-1 < \epsilon < \infty$, excluding the points $\epsilon = -1$ (purely 2D exciton) and $\epsilon = \infty$ (purely 1D exciton), we can use the hyperspherical harmonics Eq. (16) as a complete set of basic functions.²⁹ As it immediately appears from Eqs. (12) and (14), the perturbation scheme converges for $|\epsilon| < 1$. For the opposite case of $\epsilon > 1$ we can reformulate the perturbation problem with the help of the transformation $p^2 + \epsilon p_z^2 = (\epsilon + 1)[p^2 + (1/(\epsilon + 1) - 1)(p_x^2 + p_y^2)]$. After this, we can redefine the effective atomic units Eq. (2) and consider the operator $(1/(\epsilon + 1) - 1)(p_x^2 + p_y^2)$ as a perturbation, thus providing the convergence for $|1/(\epsilon + 1) - 1| < 1$.

The eigenfunctions are expanded as

$$\Psi_\nu(\alpha, \theta, \varphi) = S_\nu^{-1} \sum_s C_s^\nu \sqrt{n} \Psi_s^{(0)}(\alpha, \theta, \varphi), \quad s = (n, l, m), \quad (19)$$

where normalizing constants are defined as

$$S_\nu^2 = \sum_{n,l} C_{n,l,m}^\nu \left[n C_{n,l,m}^\nu - \sqrt{(n+l+1)(n-l)} C_{n+1,l,m}^\nu \right]. \quad (20)$$

Then, the Schrödinger equation takes the matrix form

$$\sum_{s'} \left(n \delta_{ss'} + \frac{\epsilon}{2} V_{ss'} \right) C_{s'}^\nu = \lambda_\nu C_s^\nu, \quad (21)$$

where

$$\lambda_\nu = \frac{1}{p_\nu} = \frac{1}{\sqrt{-E_\nu}}, \quad (22)$$

and the perturbation matrix is

$$V_{ss'} = \sqrt{nn'} \int \Psi_s^{(0)*}(\alpha, \theta, \varphi) (1 + \cos \alpha) \cos^2 \theta \Psi_{s'}^{(0)}(\alpha, \theta, \varphi) d^4 \Omega. \quad (23)$$

Nonvanishing matrix elements $V_{ss'}$ are (see Appendix A)

$$V_{nn'}^{ll;mm} = \mathcal{Q}_{lm} \left\{ n \delta_{nn'} + \frac{1}{2} \sqrt{(n-l)(n+l+1)} \delta_{n+1 \ n'} + \frac{1}{2} \sqrt{(n-l-1)(n+l)} \delta_{n-1 \ n'} \right\} \quad (24)$$

with

$$\mathcal{Q}_{lm} = \frac{1}{2} + \frac{1 - 4m^2}{2(2l-1)(2l+3)}, \quad (25)$$

and

$$V_{nn'}^{l \ l-2; mm} = \sqrt{\frac{[l^2 - m^2][(l-1)^2 - m^2]}{(2l+1)(2l-3)}} 2nn' \sqrt{\frac{(n-l-1)! (n'+l-2)!}{(n+l)! (n'-l+1)!}} \mathcal{F}_{nn'}^l \quad (26)$$

with

$$\mathcal{F}_{nn'}^l = \begin{cases} -1, & n' \leq n-2, \\ \frac{n-l}{2n(2l-1)} \times \begin{cases} \frac{n^2 - 4nl - l^2 + n + 3l - 2}{2(n-1)}, & n' = n-1, \\ n-l+1, & n' = n, \\ \frac{(n-l+1)(n-l+2)}{2(n+1)}, & n' = n+1, \end{cases} \\ 0, & n' \geq n+2. \end{cases} \quad (27)$$

All the other matrix elements vanish.

The perturbation method in the form of Eq. (21) is very convenient. First of all, the perturbation $\epsilon \hat{p}_z^2$ is invariant with respect to rotations around the z -axis and to the transformation $\mathbf{p} \rightarrow -\mathbf{p}$. Thus, each perturbed state has a definite parity and definite magnetic quantum number m , and the perturbation problems Eq. (21) can be solved separately for different parity and m . It implies also that the summation over s' in Eq. (21) and thereafter means that only the hydrogen states with a given parity and magnetic quantum number have to be taken into account. The time-conjugated states $\pm m$ are still degenerate. Secondly, the precise form of perturbation matrix $V_{ss'}$ provides more rigorous selection rules.

Namely, only the matrix elements with [see Eqs. (24)–(27)]

$$l' = \begin{cases} l, & n' = n, n \pm 1, \\ l - 2, & n' \leq n + 1, \\ l + 2, & n' \geq n - 1 \end{cases} \quad (28)$$

are nonvanishing.

The expansion (19) corresponds to the following coordinate representation of the anisotropic exciton wave function

$$\phi_\nu(\mathbf{r}) = \frac{p_\nu^{3/2}}{S_\nu} \sum_s C_s^\nu n^2 \phi_s^{(0)}(\mathbf{r} p_\nu n), \quad (29)$$

where $\phi_{nlm}^{(0)}(\mathbf{r})$ are the standard hydrogen wave functions. It follows from Eq. (29) that the wave function of anisotropic exciton takes the form of an infinite superposition of spherical harmonics with radially dependent coefficients. The scaling factors p_ν in the wave functions Eq. (29), which are different for different perturbed states and change adiabatically with ϵ , play the role of adiabatic scaling parameters in the perturbation theory. Moreover, the coefficients p_ν are analogous to the parameters in the Rayleigh-Ritz method. In contrast with previous works,^{11,14} where p_ν have been calculated variationally, in our approach they are strictly determined by Eq. (22). Finally, in spite of the energy scaling factors in the basis functions, the effective Hamiltonian matrix in Eq. (21) is energy independent, thus allowing for the direct diagonalization.

It can be seen from Eq. (21) that in Fock representation the spectrum of the unperturbed problem does not have a series limit. This fact is favorable for the convergence of the perturbation theory. Moreover, the spectrum is equidistant with respect to the hydrogen principal quantum number n . The matrix Eq. (24) is tridiagonal. The off-diagonal matrix elements Eq. (26) with $n' \sim n$ are rather significant but do not exceed $n/2$, i.e., they are of the order of the magnitude of the corresponding eigenvalues of the unperturbed problem. The other nonzero elements, $V_{nn'}^{l, l-2; mm} \propto n^{-l}$, decrease rapidly for fixed n' and l , and $n \gg n'$, $l > 1$. Thus, in numerical calculations we can take into account only the states with lower l , and introduce a γ -dependent upper bound for the orbital quantum number. Though the method provides a good convergence in a large region of γ , it does not allow to avoid instabilities near $\gamma = 0$ or $\gamma \rightarrow \infty$, where the perturbation scheme becomes unstable, and a strong mixing of levels occurs.

We would like to emphasize that presented perturbation method can be easily generalized for an arbitrary integer dimension $D \geq 2$ in accordance with Ref. 25, where the method of stereographic projection has been expanded to higher dimensions. In particular, for $D = 2$ the standard spherical harmonics $Y_{lm}(\theta, \varphi)$ have to be used as a basis and the operator $(\epsilon/2)\hat{V} = (\epsilon/2)(1 + \cos \theta) \cos^2 \varphi$ — as a perturbation. Here $\cos \theta = (p^2 - p_\nu^2)/(p^2 + p_\nu^2)$, $\tan \varphi = p_y/p_x$.

The problem of anisotropic exciton scattering states can be approached analogously using hyperspherical harmonics on a two-sheeted 4D-hyperboloid as a basis for the perturbation problem. The eigenvalues should be defined with positive energies, instead of Eq. (22). However, the eigenvalue problem [analogous to Eq. (21)] becomes more complicated: we have to solve now a system of integral equations, because of dependence on continuum quantum numbers.

One should note that the method of stereographic projection can be formally generalized for the fractional-dimensional exciton problem, the exciton binding energies coinciding with those obtained in Ref. 19. However, due to the generalized hyperspherical symmetry conservation (the anisotropy parameter now appears in a role of the fractional dimensionality), the energy levels are Coulomb degenerate, as it was mentioned above.

III. RESULTS AND DISCUSSIONS

Due to the symmetry properties of uniaxial anisotropic exciton Hamiltonian, matrices with even and odd l as well as with different m can be diagonalized independently. In contrast to the variational technique which provides only the upper bound of the binding energies, the Brillouin-Wigner perturbation method allows us to reach necessary precision by choosing a sufficiently large matrix to be diagonalized. We perform our calculation with a relative energy precision of 10^{-4} . In order to provide this precision in the calculation of the ground state energy for $0.6 \leq \gamma^{1/3} \leq 2$, hydrogen states with the principal quantum number up to 15 and orbital quantum number up to 6 must be taken into account. The numerical procedure becomes unstable for $\gamma \rightarrow 0$ and $\gamma \rightarrow \infty$. This non-convergency is caused by the fact that these points, where the symmetry changes (to 2D and 1D, respectively), are peculiar for the perturbation theory. The dimension change causes the levels' degeneration, when a very large (divergent) number of levels is mixed due to perturbation, and has to be

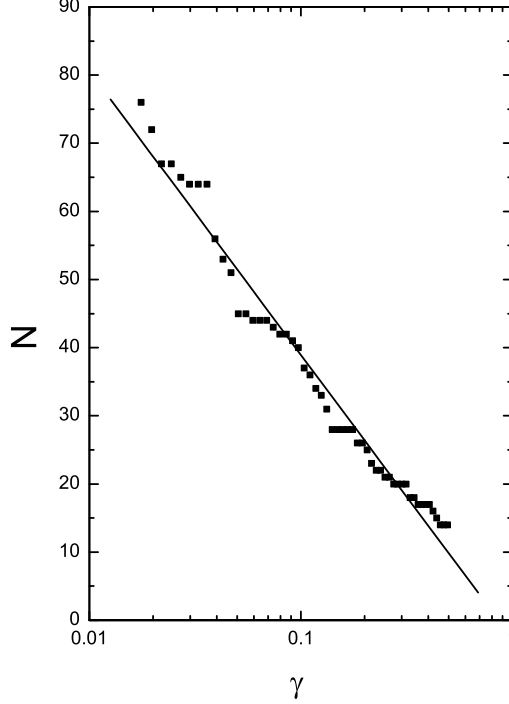


FIG. 1: The maximum principle quantum number N of the states used in numerical calculations of the ground state exciton energy within a relative margin of 10^{-4} as a function of the anisotropy parameter γ ($\gamma \leq 1$). Solid line shows the logarithmic approximation for N .

taken into account. To calculate the ground state exciton energy within a relative accuracy of 10^{-4} , the levels with principle quantum number $n \leq N$ should be taken into account. In Fig. 1 we show the numerically found dependence of N on the anisotropy parameter γ (for $\gamma \leq 1$), which is approximately logarithmic.

Note that at a rather strong anisotropy, when $\gamma \ll 1$, the ground state exciton behaves as $E_0 \approx -4 + 10.3\gamma^{1/3}$, $|\phi_0(0)|^2 \propto \gamma^{-1/3}$ and $\sqrt{\langle z^2 \rangle} \propto \gamma^{-1/3}$, (see in Ref. 3). Thus, it is useful to plot physical values in dependence on $\gamma^{1/3}$ instead of γ .

A. Energy levels

Figures 2 and 3 show the calculated eigenvalues λ_ν of Eq. (21), related to the exciton energies, $E_\nu = -1/\lambda_\nu^2$, as functions of $\gamma^{1/3}$ for $\gamma \leq 1$ (left panels); $\gamma^{-1/2}\lambda_\nu$ are shown as functions of $\gamma^{-1/3}$ for $\gamma \geq 1$ (right panels). The multiplier $\gamma^{-1/2}$ in the latter case makes the effective Rydberg finite when $\mu_\perp \rightarrow \infty$. The binding energies of $m = 0$ even parity states and $m = 1$ odd parity states are shown, respectively, in Figs. 2 and 3. Starting at $\gamma = 1$ from $\lambda_\nu = \lambda_{nml}^{(0)} = n$, all the eigenvalues with the same m and parity do not intersect when

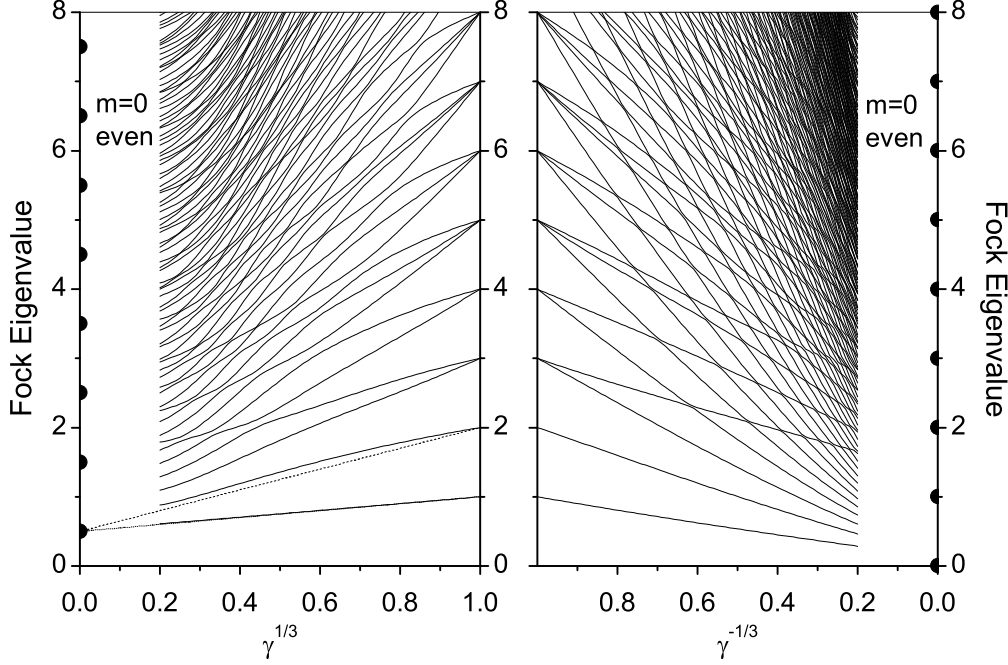


FIG. 2: Fock eigenvalues λ_ν of $m = 0$ even parity states as functions of the anisotropy parameter $\gamma^{1/3}$, $\gamma \leq 1$ (left panel), and $\gamma^{-1/2}\lambda_\nu$ as functions of $\gamma^{-1/3}$, $\gamma \geq 1$ (right panel). Solid curves never intersect each other due to a small anticrossing between the levels. The eigenvalues of purely 2D exciton (left panel) and 1D exciton (right panel) are shown by semicircles. A linear approximation of the ground and first excited state eigenvalues is plotted by dotted and dashed lines, respectively.

γ changes (multiple anticrossings occur due to the interaction between states) and approach the ground state eigenvalue of 1D exciton³⁰ $\gamma^{-1/2}\lambda_\nu \rightarrow \gamma^{-1/2}\lambda_0^{1D} \rightarrow 0$ (Figs. 2 and 3, right panels), when $\gamma \rightarrow \infty$. In the opposite case of $\gamma \rightarrow 0$ all shown eigenvalues approach the ground state eigenvalue $\lambda_0^{2D} = 1/2$ of 2D exciton ($m = 0$, Fig. 2, left panel) or the first excited state eigenvalue $\lambda_1^{2D} = 3/2$ ($m = 1$, Fig. 3, left panel). As it is clear from Fig. 2, the ground state eigenvalue dependence is almost linear over $\gamma^{1/3}$ for $\gamma \leq 1$, and

$$E_0 \approx -\frac{4}{(1 + \gamma^{1/3})^2}. \quad (30)$$

The ground state which lies much lower than the excited states almost does not interact with the latter. However, for the first excited state this interaction becomes much more significant, and its energy dependence upon $\gamma^{1/3}$ deviates from the linear one (cf. with dashed line in Fig. 2). The ratio of the energy separation between the ground state and the first excited state to the exciton binding energy is shown in Fig. 4. Starting from $3/4$ for 3D-isotropic exciton $(E_{1S} - E_{2S})/E_{1S}$ decreases monotonously with change of γ and vanishes

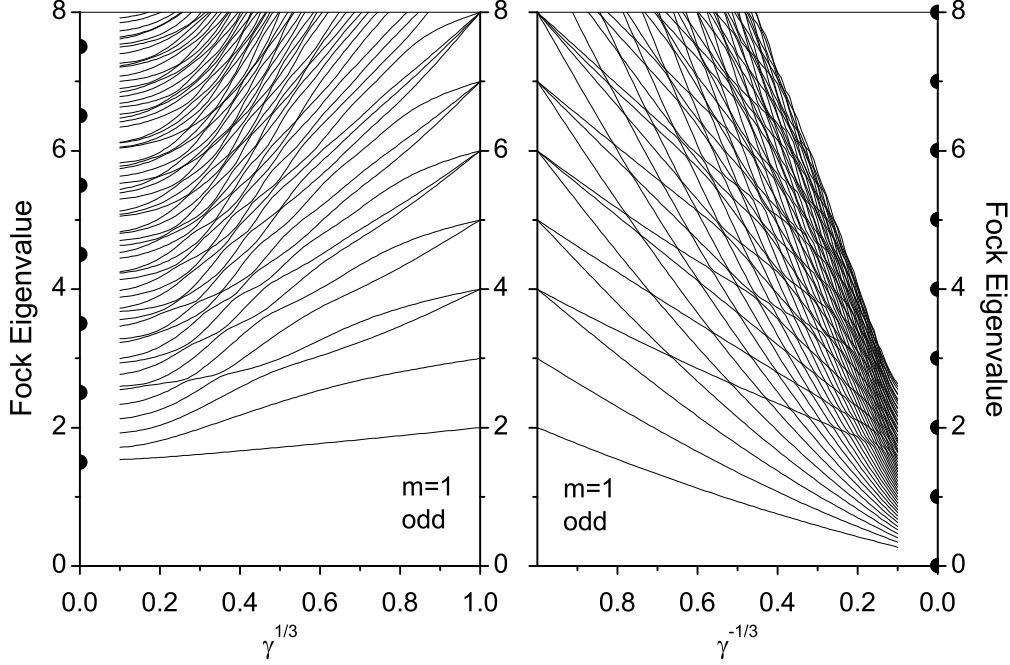


FIG. 3: Fock eigenvalues λ_ν of $m = 1$ odd parity states as functions of the anisotropy parameter $\gamma^{1/3}$, $\gamma \leq 1$ (left panel), and $\gamma^{-1/2}\lambda_\nu$ as functions of $\gamma^{-1/3}$, $\gamma \geq 1$ (right panel).

TABLE I: Exciton binding energies of several lower states calculated by means of Brillouin-Wigner perturbation method, compared with that taken from Ref. 11.

	$\gamma^{1/3}$	1S	2S	2P ₀	2P _±	3S ^a	3D ₀ ^a	3P ₀	3P _±
Ref. 11	0.8	1.233	0.3151	0.3663	0.2823	0.158	0.1375	0.1653	0.1272
This work		1.2327	0.3151	0.3664	0.2823	0.1374	0.1577	0.1652	0.1272
Ref. 11	0.4	2.01	0.695	0.933	0.3612	0.394	0.265	0.496	0.2100
This work		2.011	0.6832	0.9381	0.3615	0.2835	0.4141	0.4959	0.2107

^aThe levels classification used in the present work differs from that of Ref. 11.

when $\gamma \rightarrow 0$ or $\gamma \rightarrow \infty$. Thus, this quantity can be considered as a measure of the anisotropy of a system. Note that within the fractional dimensional model $(E_{1S} - E_{2S})/E_{1S}$ grows up as $1 - [(D - 1)/(D + 1)]^2$ (D is the dimensionality). Thus, in the anisotropic model the transition from 3D exciton to 2D or to 1D exciton differs completely from that of a system, in which the carriers localization in one or two dimensions becomes stronger and using of the fractional dimensional model is justified.

Results of our calculation for several low levels reproduce Faulkner's calculations¹¹ with

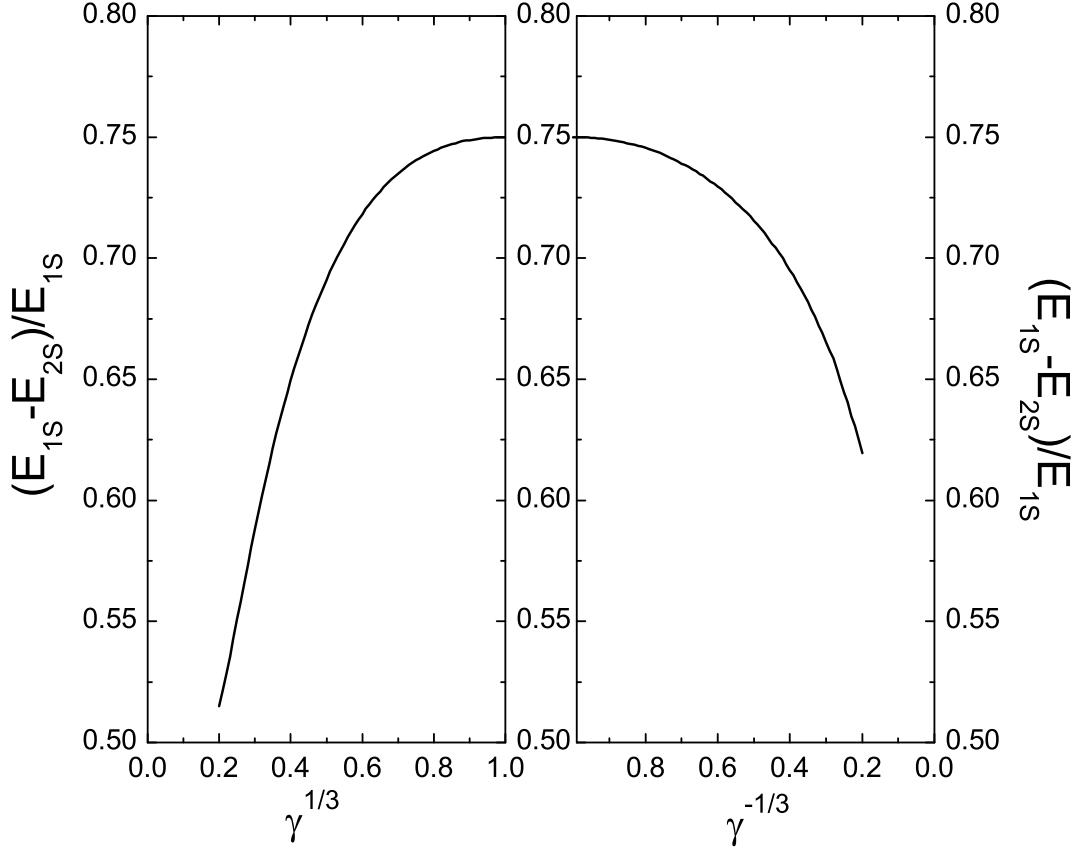


FIG. 4: The energy separation between the ground and first excited states in units of the exciton binding energy vs $\gamma^{1/3}$.

a good accuracy (see Table 1). As compared to Faulkner, we calculate a large number of excited states (up to 100 for each parity and m considered); we calculate the excitonic parameters in the region of $\gamma \leq 1$ as well as $\gamma \geq 1$, thus covering all possible values of the anisotropy parameter. Note the difference between Faulkner's and our designations of $3S$ and $3D_0$ states.³¹ When the states are split off due to perturbation, we always label the states with larger oscillator strengths at $\gamma \approx 1$ as S -state, thus establishing an order reversed to that among the states with $m \neq 0$, within our notations (see also discussions in Sec. III C and Fig. 5). Thus, at $\gamma < 1$ the $3D_0$ level lies lower than $3S$, contrary to the classification by Faulkner.¹¹ The same situation holds if we consider the higher excited states.

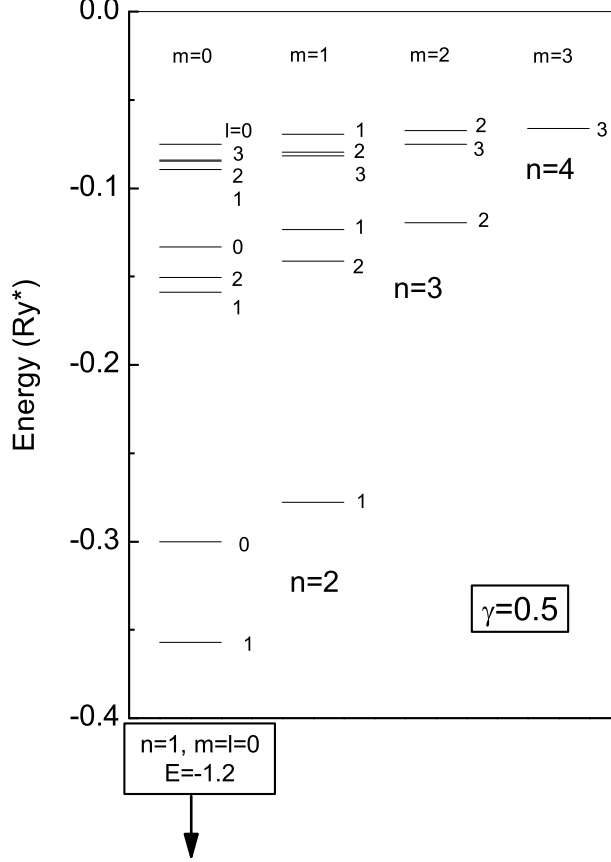


FIG. 5: Classification scheme of the energy levels of the anisotropic exciton with general quantum number $n \leq 4$ in accordance with the spherical approximation, Eq. (35). $\gamma = 0.5$.

B. Spherical approximation

Even in case of small anisotropy $|\epsilon| \ll 1$, the exciton states are linear combinations of hydrogen states with different l . However, for small ϵ the admixture of such states becomes rather small, and the accounting only for the spherically symmetric part of the perturbation proves to be very useful for understanding the evolution of levels. It is important that within such a spherical approximation, the anisotropic exciton problem is exactly soluble.

In this section we consider the approximate solution of the anisotropic exciton problem in a form $\psi(\mathbf{r}) = R(r)Y_{lm}(\theta, \varphi)$, thus taking into account only diagonal in l parts of the perturbation, Eqs. (24),(25), and neglecting the perturbation matrix elements mixing different spherical harmonics.

In order to neglect $l \neq l'$ matrix elements, let us replace in the Schrödinger equation,

Eq. (6), the operator \hat{p}_z^2 by the operator \hat{Q} , defined as

$$\hat{Q}Y_{lm}(\theta, \varphi) = p^2 \mathcal{Q}_{lm} Y_{lm}(\theta, \varphi), \quad (31)$$

$$\mathcal{Q}_{lm} = \int \cos^2 \theta |Y_{lm}(\theta, \varphi)|^2 d^3 \Omega \quad (32)$$

[see also Eq. (25)]. Then, after the substitution

$$p \rightarrow \frac{p}{1 + \epsilon \mathcal{Q}_{lm}}, \quad p_\nu^2 \rightarrow \frac{p_\nu^2}{1 + \epsilon \mathcal{Q}_{lm}}, \quad (33)$$

which, in fact, corresponds to a (l, m) -dependent mass renormalization, we arrive at a symmetrical (unperturbed) Schrödinger equation with the solution

$$\phi_\nu(\mathbf{r}) = (1 + \epsilon \mathcal{Q}_{lm})^{-3/2} \phi_{nlm}^{(0)} \left(\frac{\mathbf{r}}{1 + \epsilon \mathcal{Q}_{lm}} \right), \quad (34)$$

$$E_\nu = -\frac{1}{n^2(1 + \epsilon \mathcal{Q}_{lm})}, \quad (35)$$

in units of Eq.(2) and with the use of dilatation of z .

One can easily see from Eq. (34) that in this spherical approximation the perturbation compresses (for $\epsilon < 0$) or dilates (for $\epsilon > 0$) the scale of a given hydrogen wave function by the factor $1 + \epsilon \mathcal{Q}_{lm}$, which is different for different spherical harmonics. Note, that the hidden hydrogen-like symmetry is broken within this spherical approximation, and the binding energies now depend on l and m . However, the spectrum Eq. (35) still has a hydrogen-like dependence on the principle quantum number n .

In Fig.5 we show schematically the energy levels of anisotropic exciton, calculated via Eq. (35) for $\gamma = 0.5$, $n \leq 4$ and all possible l and m . Equation (35) provides a correct qualitative description of the levels evolution and is in agreement with the result of calculations presented in Sec. III A in the vicinity of $\gamma = 1$ (see Fig. 6).

The accounting for $l \neq l'$ matrix elements (in case of small ϵ) yields correct quadratic in ϵ terms in the energies. The rational form of matrix elements Eqs. (26) and (27) allows us to sum up the standard perturbation theory series in the second order. The calculated in the second order exciton binding energies of several lower levels are given in Appendix A [see Eq. (A17)], their dependence on γ is also illustrated in Fig.6 (dashed lines).

C. Oscillator strengths

Within the envelope function approximation, the relative oscillator strengths of dipole-allowed transitions f_ν are proportional to $|\phi_\nu(0)|^2$ (see, e.g., in Ref. 32). Bearing in mind

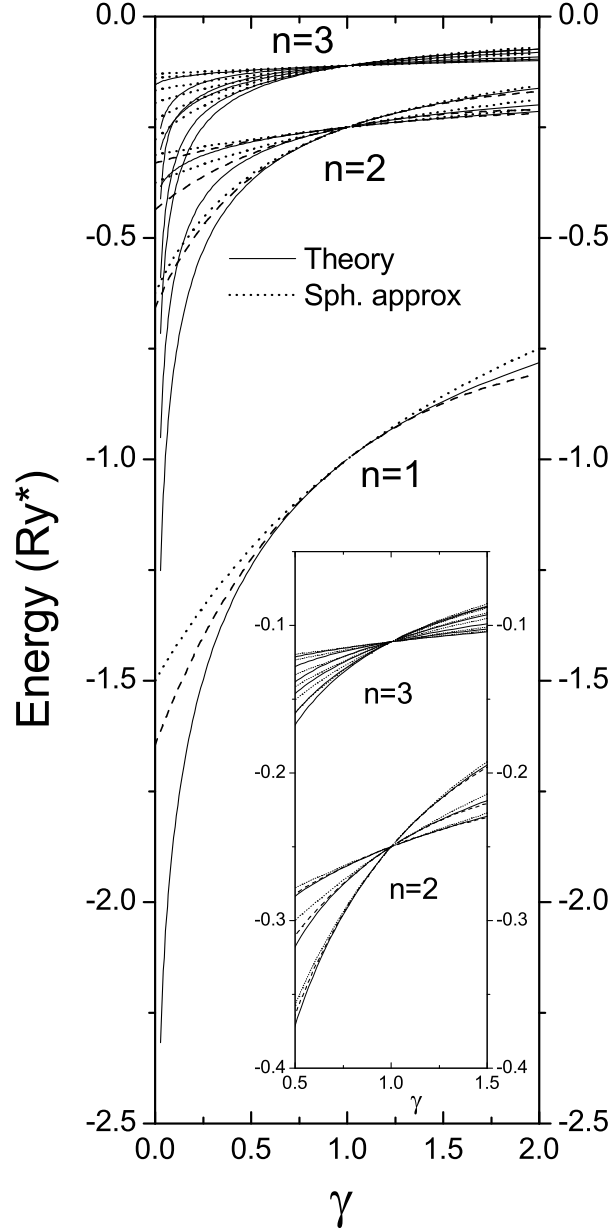


FIG. 6: Lower energy levels as functions of $\gamma^{1/3}$, calculated by means of the perturbation method (solid curves), within the spherical approximation (dotted lines), and in the 2nd order perturbation theory approximation (dashed curves).

the expansion of Eq. (29) and the fact that for the unperturbed states $\phi_\nu(0) \neq 0$ only for $l = m = 0$, we get

$$f_\nu \propto |\phi_\nu(0)|^2 = \frac{p_\nu^3}{\pi S_\nu^2} \left| \sum_n C_{n,0,0}^\nu \sqrt{n} \right|^2. \quad (36)$$

Figure 7 shows the calculated numerically oscillator strengths of lower S , D_0 and G_0 -like states as functions of the anisotropy parameter. It is seen in Fig.7 that the oscillator

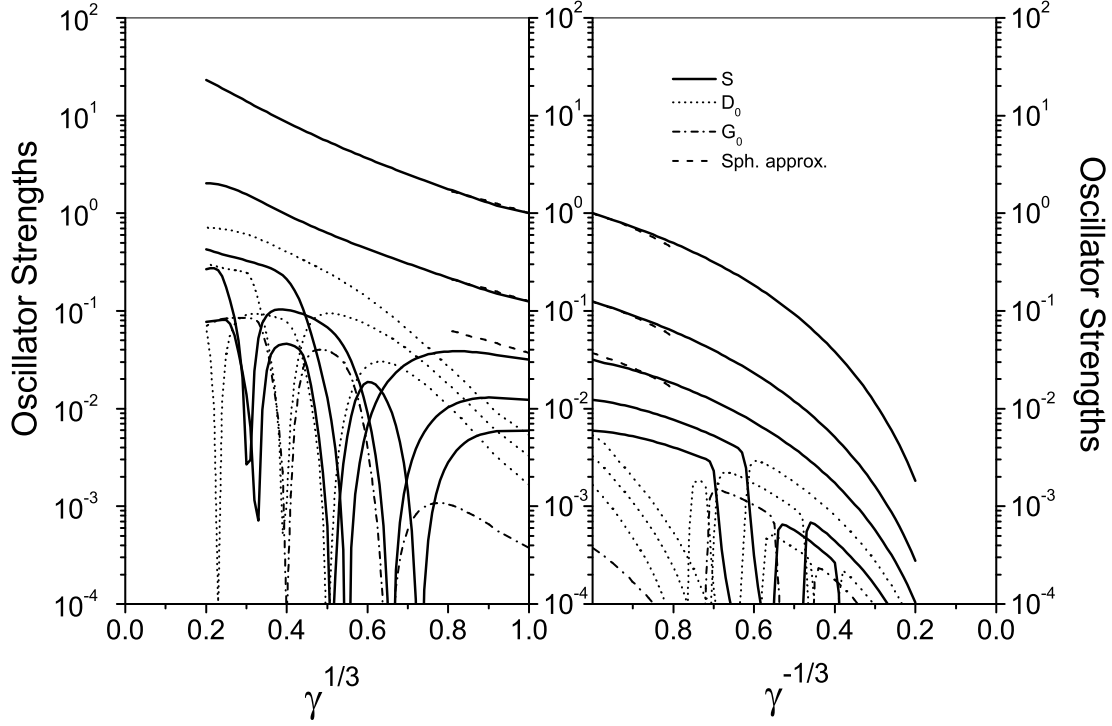


FIG. 7: The anisotropic exciton oscillator strengths of lower S , D_0 and G_0 -like states as functions of the anisotropy parameter $\gamma^{1/3}$, calculated numerically and within the spherical approximation (in units of the ground state oscillator strength at $\gamma = 1$). Within the spherical approximation, the oscillator strengths of D_0 and G_0 -like states are vanishing.

strengths of all shown states do not vanish at $\gamma = 1$. Originated from the degenerate states of isotropic 3D exciton, the perturbed states become fixed linear combinations of the former even when the perturbation tends to zero. It can be explained as follows. The perturbation of a symmetry lower than the original Hamiltonian implies the existence of strictly definite combinations of basis functions for degenerate states when $\gamma = 1$, while the symmetry of the unperturbed Hamiltonian allows an arbitrary choice of these combinations. At $\gamma \approx 1$ S -like state is optically more intensive than D_0 -like state. The picture changes drastically with the increase of anisotropy. Near $\gamma^{1/3} = 0.8$ the oscillator strength of $3D_0$ state overcomes that of $3S$ one. For $\gamma^{1/3} < 0.8$ the intensity of the $3S$ state collapses due to the interaction with $4D_0$ state and then revives after interaction with higher levels. Moreover, the anisotropy increase leads to substantial growth of the oscillator strengths of higher excited states, such as $4S$ and $4D_0$, making them optically significant. Similar situation takes place if $\gamma > 1$ (when a transition from 3D to 1D exciton occurs). Such a redistribution of the oscillator

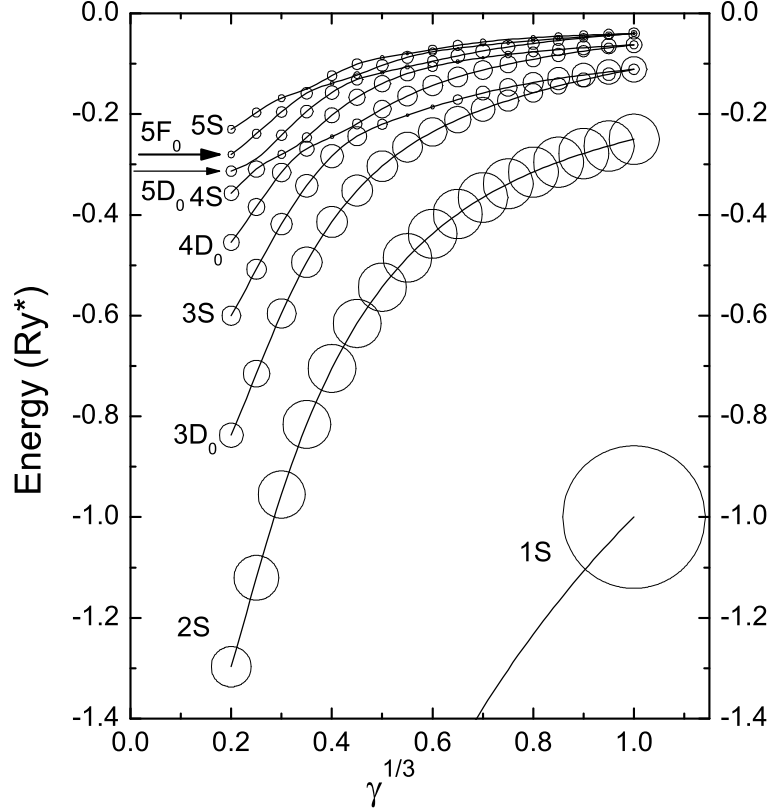


FIG. 8: Energies and oscillator strength of excited optically active states vs $\gamma^{1/3}$ ($\gamma \leq 1$). The area of a circle is equal to the oscillator strength, normalized to the ground state oscillator strength, which is taken constant for all γ , see a single circle on the bottom (ground state) curve.

strengths between different states is due to multiple uncrossings between energy levels interacting with each other. This effect can be clearly seen in Fig. 8, where the area of a circle placed on the energy curve is proportional to the oscillator strength of a given excited state, normalized to the ground state oscillator strength.

Within the spherical approximation, as it follows from Eq. (34),

$$f_\nu = \left(1 + \frac{\epsilon}{3}\right)^{-3} f_\nu^{(0)}, \quad (37)$$

where $f_\nu^{(0)} = 1/n^3$ are the oscillator strengths of the isotropic exciton (in units of $f_{1S}^{(0)}$). The oscillator strengths of $1S$, $2S$ and $3S$ states calculated according to Eq. (37) are displayed in Fig. 7 by dashed lines. Note that the oscillator strengths of $3S$ state, calculated numerically and within the spherical approximation, do not coincide at $\gamma = 1$, as the spherical approximation does not reflect correctly the symmetry violation in the vicinity of this point. However, the sum of the oscillator strengths of $3S$ and $3D_0$ levels is equal to $1/3^3$.

IV. CONCLUSIONS

The perturbation theory of anisotropic exciton is developed based of the Fock transformation. This transformation depends on the exciton energies as adiabatic parameters and admits a separation of bound and scattering exciton states. For the bound states the eigenfunctions are expanded into a complete set of hyperspherical harmonics on a 4D-sphere, creating a representation of the full symmetry group $O(4)$ of hydrogen-like system, and the perturbation matrix elements acquire an explicit algebraic form. This allows us to analytically perform a partial diagonalization of the Hamiltonian matrix. It results in a spherical approximation which proves to be very useful for levels evolution analysis. The eigenvalues and eigenvectors are found by a numerical diagonalization of the effective Hamiltonian matrix. The energies and oscillator strengths of anisotropic exciton states are calculated for all values of the anisotropy parameter $0 < \gamma < \infty$ (including both flattened and elongated excitons), except the vicinities of $\gamma = 0$ and $\gamma = \infty$ where the dimensionality of the system changes, respectively, to $D = 2$ and to $D = 1$. It is found that with the increase of the anisotropy a strong redistribution of oscillator strengths between optically active and formerly inactive states occurs: the oscillations in optical intensities of higher excited states take place, and the switching on of formerly weak optical transitions is predicted.

Acknowledgments

The authors are thankful to R. Zimmermann for critical reading of the manuscript, useful discussions which helped us to clarify the question of completeness of the basis used in our perturbation method, and for helpful advices. This work was supported by Russian Basic Research Foundation, Russian Ministry of Science (program “Nanostructures”), and INTAS (grant #96-0398). A. E. B. was supported by the Dissertation Fellowship from CUNY.

Appendix A: Perturbation matrix. Exciton binding energies in the second order approximation

Due to a separation of variables, the matrix element $V_{ss'}$, Eq. (23), takes the form

$$V_{nn'}^{ll';mm'} = \mathcal{J}_{ll'}^{mm'} \mathcal{I}_{nn'}^{ll'} \sqrt{nn'}, \quad (\text{A1})$$

where

$$\mathcal{J}_{ll'}^{mm'} = \delta_{mm'} \mathcal{N}_{lm} \mathcal{N}_{l'm} \int_{-1}^1 P_l^m(x) P_{l'}^m(x) x^2 dx, \quad (\text{A2})$$

$$\mathcal{N}_{lm} = \left[\frac{(2l+1)}{2} \frac{(l-|m|)!}{(l+|m|)!} \right]^{1/2}, \quad (\text{A3})$$

$$\mathcal{I}_{nn'}^{ll} = \mathcal{D}_{nl}^* \mathcal{D}_{n'l} \int_{-1}^1 (1-x^2)^{l+\frac{1}{2}} (1+x) C_{n-l-1}^{l+1}(x) C_{n'-l-1}^{l+1}(x) dx, \quad (\text{A4})$$

$$\mathcal{D}_{nl} = (-2i)^l l! \sqrt{\frac{2n(n-l-1)!}{\pi(n+l)!}}. \quad (\text{A5})$$

Using the recurrent relations

$$(2l+1)xP_l^m = (l-m+1)P_{l+1}^m + (l+m)P_{l-1}^m, \quad (\text{A6})$$

$$2(\nu+\alpha)x C_\alpha^\nu(x) = (\alpha+1)C_{\alpha+1}^\nu(x) + (2\nu+\alpha-1)C_{\alpha-1}^\nu(x), \quad (\text{A7})$$

and normalization property for Legendre (P_l^m) and Gegenbauer (C_α^ν) polynomials we get

$$\begin{aligned} \mathcal{J}_{ll'}^{mm'} = \delta_{mm'} \left\{ \frac{1}{2} \left[1 + \frac{1-4m^2}{(2l-1)(2l+3)} \right] \delta_{l \ l'} + \frac{1}{2l-1} \sqrt{\frac{[l^2-m^2][(l-1)^2-m^2]}{(2l+1)(2l-3)}} \delta_{l-2 \ l'} \right. \\ \left. + \frac{1}{2l+3} \sqrt{\frac{[(l+1)^2-m^2][(l+2)^2-m^2]}{(2l+1)(2l+5)}} \delta_{l+2 \ l'} \right\} \quad (\text{A8}) \end{aligned}$$

and

$$\mathcal{I}_{nn'}^{ll} = \delta_{nn'} + \frac{1}{2} \sqrt{\frac{(n-l)(n+l+1)}{n(n+1)}} \delta_{n+1 \ n'} + \frac{1}{2} \sqrt{\frac{(n+l)(n-l-1)}{n(n-1)}} \delta_{n-1 \ n'}. \quad (\text{A9})$$

To derive matrix elements $\mathcal{I}_{nn'}^{ll\pm 2}$ we use the tabulated integral²⁴

$$\frac{2}{\pi} \int_{-1}^1 (1-x)^{-1} (1-x^2)^{\nu-\frac{1}{2}} C_m^\nu(x) C_n^\nu(x) dx = \frac{2}{\sqrt{\pi}} \frac{\Gamma(\nu-\frac{1}{2})}{\Gamma(\nu)} C_m^\nu(1), \quad m \leq n, \quad (\text{A10})$$

where

$$C_m^\nu(1) = \frac{(m+2\nu-1)!}{(2\nu-1)!m!}, \quad \nu \neq 0, \quad C_m^0(1) = \frac{2}{m}, \quad m \neq 0. \quad (\text{A11})$$

$$\mathcal{I}_{nn'}^{ll-2} = \mathcal{D}_{nl}^* \mathcal{D}_{n'l-2} \int_{-1}^1 (1-x^2)(1+x)^{l-\frac{1}{2}} (1-x)^{l-\frac{3}{2}} C_{n-l-1}^{l+1}(x) C_{n'-l+1}^{l-1}(x) dx. \quad (\text{A12})$$

Using Eq. (A7) and the recurrent relations

$$2\nu(1-x^2)C_{\alpha-2}^{\nu+1}(x) = (\alpha+2\nu-1)x C_{\alpha-1}^\nu(x) - \alpha C_\alpha^\nu(x), \quad (\text{A13})$$

$$\alpha C_\alpha^{\nu-1}(x) = 2(\nu-1) [x C_{\alpha-1}^\nu(x) - C_{\alpha-2}^\nu(x)], \quad (\text{A14})$$

we are able to write the integral in Eq. (A12) in the form of Eq. (A10),

$$\mathcal{I}_{nn'}^{ll-2} = \mathcal{D}_{nl}^* \mathcal{D}_{n'l-2} \frac{l-1}{l} \int_{-1}^1 (1+x)^{l-\frac{1}{2}} (1-x)^{l-\frac{3}{2}} (\xi_{nl} C_{n-l-1}^l - \eta_{nl} C_{n-l+1}^l) (C_{n'-l-1}^l - C_{n'-l+1}^l) dx, \quad (\text{A15})$$

where

$$\xi_{nl} = \frac{(n+l)(n+l-1)}{4nn'}, \quad \eta_{nl} = \frac{(n-l)(n-l+1)}{4nn'}. \quad (\text{A16})$$

After simple transformations we arrive to Eqs. (24)–(27).

Note that we are able to apply the standard Reley-Schrödinger perturbation theory to Eq. (21) and to calculate analytically the perturbation theory corrections (to nondegenerate levels) of a given order, due to the rational form of the perturbation matrix elements Eqs. (24)–(27). For example, for several lower levels the accounting for the perturbation theory terms up to the second order inclusive leads to

$$\begin{aligned} E_{1S} &= -\frac{1}{\left[1 + \frac{1}{6}\epsilon + \left(\frac{\pi^2}{45} - \frac{59}{216}\right)\epsilon^2\right]^2}, & E_{2S} &= -\frac{1}{4\left[1 + \frac{1}{6}\epsilon + \left(-\frac{4\pi^2}{45} + \frac{173}{216}\right)\epsilon^2\right]^2}, \\ E_{2P_0} &= -\frac{1}{4\left[1 + \frac{3}{10}\epsilon + \left(\frac{4\pi^2}{35} - \frac{25441}{21000}\right)\epsilon^2\right]^2}, & E_{2P_{\pm}} &= -\frac{1}{4\left[1 + \frac{1}{10}\epsilon + \left(\frac{8\pi^2}{105} - \frac{49307}{63000}\right)\epsilon^2\right]^2}. \end{aligned} \quad (\text{A17})$$

* Electronic address: muljarov@gpi.ru

² C. Kittel and A. Mitchell, Phys. Rev. **96**, 1488 (1954).

³ W. Kohn and J. M. Luttinger, Phys. Rev. **98**, 915 (1955).

⁴ G. Bastard, *Wave Mechanics Applied to Semiconductor Heterostructures* (Les Editions de Physique, Les Ulis, France, 1988), p. 26.

⁵ M. F. Pereira Jr., I. Galbraith, S. W. Koch, and G. Duggan, Phys. Rev. B **42**, 7084 (1990).

⁶ Partha Ray and P. K. Basu, Phys. Rev. B **47**, 15958 (1993).

⁷ J. J. Hopfield and D. G. Thomas, Phys. Rev. **122**, 35 (1961).

⁸ R. G. Wheeler and J. O. Dimmock, Phys. Rev. **125**, 1805 (1962).

⁹ J. A. Deverin, Nuovo Cimento B **63**, 1 (1969).

¹⁰ B. Segal, Phys. Rev. **163**, 769 (1967).

¹¹ R. A. Faulkner, Phys. Rev. **184**, 713 (1969).

¹² O. Akimoto and H. Hasegawa, J. Phys. Soc. Jpn. **22**, 181 (1967).

¹³ E. O. Kane, Phys. Rev. **180**, 852 (1969).

- ¹⁴ A. Baldereschi and M. G. Diaz, *Nuovo Cimento B* **68**, 217 (1970).
- ¹⁵ R. Zimmermann, *Phys. Stat. Sol. (b)* **46**, K111 (1971).
- ¹⁶ Jian-Bai Xia, *Phys. Rev. B* **39**, 5386 (1989).
- ¹⁷ J. Deppe, M. Balcanski, R. F. Wallis, and K. P. Jain, *Sol. State Commun.* **84**, 67 (1992).
- ¹⁸ As it immediately follows from the form of the anisotropic exciton Hamiltonian [see Eq. (1)], through a substitution of variables one can make isotropic either the kinetic or the potential energy.
- ¹⁹ X. F. He, *Phys. Rev. B* **42**, 11751 (1990); **43**, 2063 (1991).
- ²⁰ Ch. Tanguy, P. Lefebvre, H. Mathieu, and R. J. Elliot, *Phys. Stat. Sol. (a)* **164**, 159 (1997).
- ²¹ M. F. Pereira Jr., *Phys. Rev. B* **52**, 1978 (1995).
- ²² A short description of our method see in: E. A. Muljarov, A. L. Yablonskii, S. G. Tikhodeev A. E. Bulatov and Joseph L. Birman, *Phys. Rev. B*, to be published (1999).
- ²³ V. A. Fock, *Zh. Physik* **98**, 145 (1935).
- ²⁴ I. S. Gradshtein and I. M. Ryzhik, *Tables of Integrals, Series, and Products* (Academic, New York, 1980).
- ²⁵ M. Bander and C. Itzykson, *Rev. Mod. Phys.* **38**, 330 (1966); **38**, 346 (1966).
- ²⁶ It can be shown that $\int \cos \alpha |\Psi_{nlm}^{(0)}|^2 d^4\Omega = 0$.
- ²⁷ B. Podolansky and L. Pauling, *Phys. Rev.* **34**, 109 (1929).
- ²⁸ L. D. Landau and E. M. Lifchitz, *Quantum Mechanics. Nonrelativistic Theory* (Pergamon Press, New York, 1976).
- ²⁹ For instance, in the coordinate representation the *S*-type basic functions are proportional to $\exp(-p_\nu r) L_n^1(2p_\nu r)$ instead of $\exp(-r/n) L_n^1(2r/n)$, thus forming a complete set for spherically symmetric functions [See also Eq. (29)].
- ³⁰ It is well known that in exactly 1D case the ground state exciton energy is infinite (logarithmically diverges). See, e.g., in Ref. 28.
- ³¹ The standard quantum numbers n, l and hydrogen-like notations can be used in case of the anisotropic exciton only approximately.
- ³² G. Dresselhaus, *Phys. Rev.* **106**, 76 (1957).